




Two Sides of the Same Coin: Tendoligamentous Similarities and Dissimilarities of Great Toe and Thumb Anatomy on MRI

Heena Rajani¹ Dharmendra Kumar Singh¹  Saurabh Suman¹ Amit Katyan¹ Anuradha Sharma¹
Nishith Kumar¹

¹Department of Radio-diagnosis, Vardhman Mahavir Medical College and Safdarjung Hospital, New Delhi, India

Address for correspondence Dharmendra Kumar Singh, MD, FRCR, Department of Radio-diagnosis, Vardhman Mahavir Medical College and Safdarjung Hospital, New Delhi, India 110029 (e-mail: dksinghrad@gmail.com).

Indian J Radiol Imaging 2022;32:113–123.

Abstract

Evolution and functional necessities have compelled the great toe of the foot and its embryological kin, thumb, to have some tendoligamentous differences with a similar basic anatomical structure. This provides biomechanical advantage to these joints: the thumb is apposable and more mobile, ensuring hand dexterity and tool-handling, whereas the great toe is less mobile and more stable, ensuring weight bearing, strength, and stability for bipedal locomotion. This pictorial review will methodically illustrate the similarities and dissimilarities of the joint morphology and its tendoligamentous attachments at the level of carpometacarpal joint, metacarpophalangeal joint, and interphalangeal joints of thumb compared with tarsometatarsal joint, metatarsophalangeal joint, and interphalangeal joints of great toe. It intends to provide a comprehensive understanding of the normal anatomy of great toe and thumb to the radiologists, enabling better interpretation of the pathologies.

Keywords

- ▶ MRI
- ▶ great toe
- ▶ thumb
- ▶ hallux
- ▶ pollicis

Introduction

With evolution, quadrupeds progressed to develop two hands and two feet. Driven by functional necessity, thumb evolved to become opposable for maintaining hand dexterity, and great toe evolved to optimize weight bearing, balance, and bipedal locomotion.¹ Therefore, there are anatomical tendoligamentous modifications at the level of carpometacarpal (CM) joint and metacarpophalangeal (MCP) of thumb compared with tarsometatarsal (TM) joint, and metatarsophalangeal (MTP) joint of great toe. Understanding the anatomical modifications is essential to analyze the anatomy and biomechanics of these joint on magnetic resonance imaging (MRI) that will aid in comprehensive evaluation of the patterns of injury in these joints.

In addition to limited range of movements in the joints of great toe, another major difference between great toe and thumb is that the coronal plane of thumb is nearly at right angle to that of the rest of the fingers and rotated medially, whereas the great toe lies in the same coronal plane as the rest of the toe² (▶ **Fig. 1**).

In the current pictorial review, we will illustrate the radiological anatomy of thumb and great toe on 3T MRI. The capsuloligamentous anatomy and tendinous attachments will be described at the level of TM/CM joint, MTP/MCP, and interphalangeal (IP) joints highlighting similarities and dissimilarities at each level.

For the great toe MRI, the patient is placed in supine position, the plantar surface of foot flat against bottom of foot coil, and the foot at 90 degrees to leg. The sequences,

published online
April 19, 2022

DOI <https://doi.org/10.1055/s-0042-1743114>.
ISSN 0971-3026.

© 2022. Indian Radiological Association. All rights reserved.
This is an open access article published by Thieme under the terms of the Creative Commons Attribution-NonDerivative-NonCommercial-License, permitting copying and reproduction so long as the original work is given appropriate credit. Contents may not be used for commercial purposes, or adapted, remixed, transformed or built upon. (<https://creativecommons.org/licenses/by-nc-nd/4.0/>)
Thieme Medical and Scientific Publishers Pvt. Ltd., A-12, 2nd Floor, Sector 2, Noida-201301 UP, India

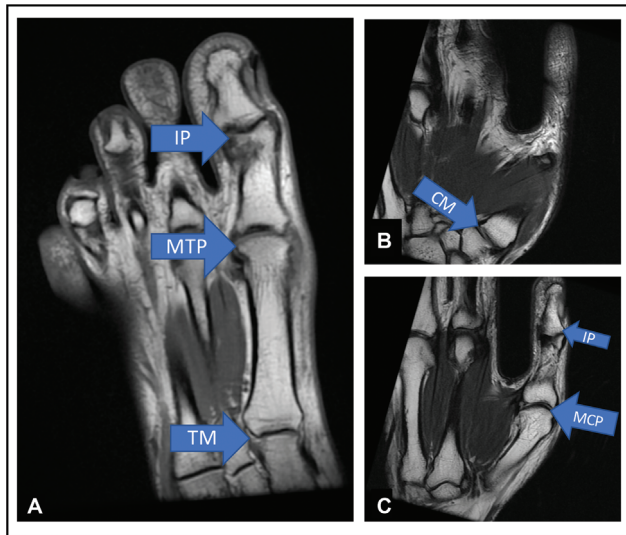


Fig. 1 Overview of the joints of great toe and thumb. (A) Axial T1-weighted (T1W) magnetic resonance (MR) image shows that the great toe lies in the same plane as the rest of the toe. The tarsometatarsal (TM) joint, metatarsophalangeal (MTP) joint, and interphalangeal (IP) joint are marked. (B and C). Serial sagittal T1W MR image of the thumb shows that the thumb lies at almost ninety degrees to the plane of the rest of the fingers and is rotated medially. The first carpometacarpal (CM) joint, metacarpophalangeal (MCP) joint, and IP joint are marked.

Table 1 Scan sequences and parameters of great toe

| Sequence | Plane | Slice thickness | FOV (cmx cm) |
|----------|----------|-----------------|--------------|
| PDFS | Axial | 2–3 | 8 × 16 |
| PDFS | Coronal | 2–3 | 12 × 10 |
| PDFS | Sagittal | 2–3 | 18 × 10 |
| T1W | Sagittal | 2–3 | 18 × 10 |
| T2W | Coronal | 2–3 | 12 × 10 |

Abbreviations: FOV, field of view; PDFS, fat suppressed proton density; T1W, T1-weighted.

planes, and scan parameters are summarized in ►Table 1 and the planning is summarized in ►Fig. 2. For the thumb MRI, patient is placed in prone position with elevated arm (super-

Table 2 Scan sequences and parameters of thumb

| Sequence | Plane | Slice thickness | FOV (cmxcm) |
|----------|----------|-----------------|-------------|
| PDFS | Axial | 2–3 | 8 × 8 |
| PDFS | Coronal | 2–3 | 10 × 12 |
| PDFS | Sagittal | 2–3 | 10 × 12 |
| T1W | Sagittal | 2–3 | 10 × 12 |
| T2W | Coronal | 2–3 | 10 × 12 |

Abbreviations: FOV, field of view; PDFS, fat suppressed proton density; T1W, T1-weighted.

man position), with the thumb placed in fully extended position at the center of the scanner. The sequences, planes, and scan parameters are summarized in ►Table 2 and the planning is summarized in ►Fig. 3.

Tarsometatarsal/Carpometacarpal Joints

Great Toe

The first TM joint of foot forms the medial column of the Lisfranc’s joint that provides stability to the mid foot and forefoot. It is an arthrodial joint between the distal articular surface of the medial cuneiform and the base of first metatarsal, allowing flexion and extension with limited abduction and rotation. The dorsomedial ligament connects the dorsal surface of the medial cuneiform to that of base of first metatarsal, the dorsal Lisfranc’s ligament extends from the dorsolateral side of medial cuneiform to the medial surface of base of second metatarsal, and the dorsal intercuneiform ligament connects the medial and intermediate cuneiforms. The plantar TM ligament and the plantar Lisfranc’s complex connects plantar surface of medial cuneiform to plantar surface of base of first, second, and third metatarsal, respectively. The tendon of tibialis anterior attaches on the medioplantar aspect of the base of first metatarsal and the distal end of medial cuneiform, whereas the peroneus longus attaches on the lateral aspect of the same^{3,4} (►Fig. 4).

The Lisfranc’s ligament is responsible for anterolateral stabilization of midfoot and forefoot. As

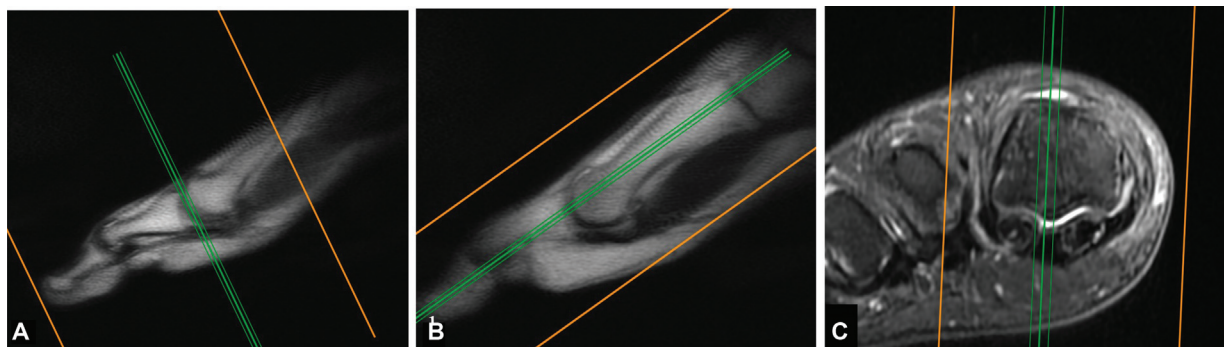


Fig. 2 Planning of magnetic resonance imaging great toe. (A) First, the localizer was used to plan axial images perpendicular to the long axis of the metatarsal and proximal phalanx. (B) The coronal slices were planned on the sagittal plane, parallel to the to the long axis of the metatarsal and proximal phalanx. (C) Using axial images, sagittal scan was planned perpendicular to the line joining the two sesamoids.

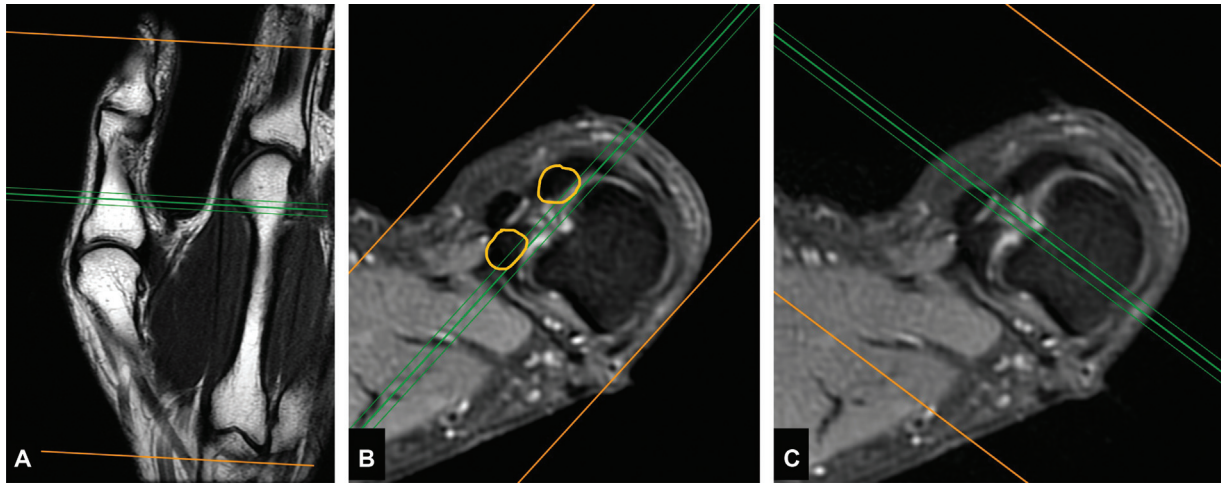


Fig. 3 Planning of magnetic resonance imaging thumb. (A) First, localizer was used to plan axial images perpendicular to the long axis of the proximal phalanx. (B) Using axial images, coronal scan was planned parallel to the line joining the two sesamoids (outlined with yellow circle). (C) Using axial images, sagittal scan was planned perpendicular to the line joining the two sesamoids.

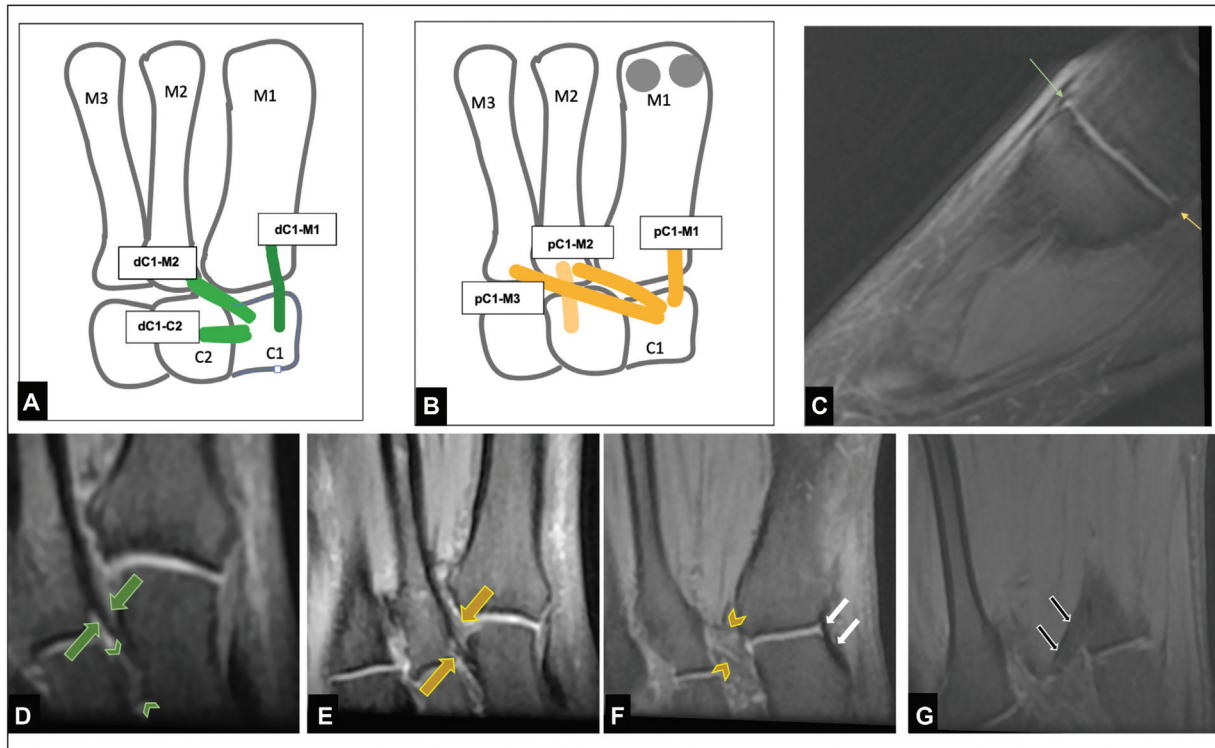


Fig. 4 Ligaments around first tarsometatarsal joint. (A) Diagrammatic representation of the three dorsal ligaments: dorsomedial ligament (dC1-M1) that is between dorsal surface of medial cuneiform (C1) and the dorsal surface of the base of first metatarsal (M1), proper Lisfranc's ligament (dC1-M2) between the dorsal surface of medial cuneiform (C1) and base of second metatarsal (M2) and the intercuneiform ligament (dC1-C2) between the dorsal surfaces of the medial (C1) and intermediate cuneiform (C2). (B) Diagrammatic representation of the three plantar ligaments: plantar tarsometatarsal ligament (pC1-M1) between plantar surface of medial cuneiform (C1) to base of first metatarsal (M1) and the proper plantar Lisfranc's ligament's complex (pC1-M2/M3) extending between medial cuneiform and plantar surface of base of second (M2) and third metatarsal (M3). (C) Sagittal fat suppressed proton density (PDFS) weighted magnetic resonance image shows dorsomedial ligament (thin green arrow) and plantar tarsometatarsal ligament (thin yellow arrow). (D-G) Serial axial PDFS image from dorsal to plantar aspect shows proper dorsal ligament (thick green arrows, D) and intercuneiform ligament (green arrow heads, D), pC1-M2 (thick yellow arrow, E) and pC1-M3 (yellow arrow heads, F) components of proper plantar Lisfranc ligament. The tendon of tibialis anterior (white arrows, F) can be seen attaching to the base of distal phalanx and the adjacent proximal aspect of medial cuneiform. The tendon of the peroneus longus (black arrows, G) can be seen attaching to the lateral aspect of base of the first metatarsal.

anterolateral stabilization is not required in thumb, the corresponding Lisfranc's akin ligament is not seen in the thumb.⁵

Thumb

The first CM joint is an incongruous saddle joint between trapezium and first metacarpal with a wide range of motion, including flexion, extension, abduction, adduction, and circumduction, contributing to the apposable and prehensile capability of the human thumb. There are five main ligaments around this joint, divided into dorsal and volar group. The ligaments of the dorsal group include dorsoradial ligament (DRL), posterior oblique ligament (POL), collectively called dorsal carpometacarpal ligament complex as-well-as intermetatarsal ligament (IML). They are best visualized in the sagittal plane, except IML that is seen on oblique coronal reformatted image across the first web space. DRL is a capsular ligament that extends from the dorsoradial tubercle of trapezium to the dorsolateral surface of base of first metacarpal, attaching deep to the attachment of abductor pollicis longus (APL) tendon. POL is also a capsular ligament, attached more ulnar to the DRL. IML connects the base of the first and second metacarpals. The volar trapeziometacarpal ligament includes the anterior oblique ligament (AOL—superficial capsular and deep intracapsular components) extending from the volar tubercle of trapezium to the volar tubercle of the base of first metacarpal and the ulnar collateral ligament, a thin ligament on the ulnar aspect of AOL that is often difficult to appreciate, separately from AOL, on MRI.^{6,7} The tendon of APL attaches to the radial aspect of base of the first metacarpal³ (→Fig. 5 and →Table 3).

Metatarsophalangeal/ Metacarpophalangeal Joints

Great Toe

The first MTP joint is an ellipsoid joint between the head of first metatarsal and base of first proximal phalanx that allows flexion, extension, limited adduction, abduction, rotation, and circumduction. There exists a “plantar plate complex” that stabilizes and protects the joint, aiding in propulsion while walking and maintaining balance. It comprises the sesamoido-capsulo-ligamentous complex and a musculo-tendinous complex.⁸

There are two sesamoid bones, medial and lateral, articulating in the respective grooves present on the plantar surface of the first metatarsal head. They function as a pulley system, providing attachment and smooth movement of tendons as well as protection to the underlying joint. The sesamoids are connected to each other by the intersesamoid ligament (ISL), to the base of proximal phalanx by the paired sesamoidophalangeal ligaments (SPL) and to the plantar aspect of first metatarsal neck by the paired metatarsosesamoid ligaments. The SPLs are thicker

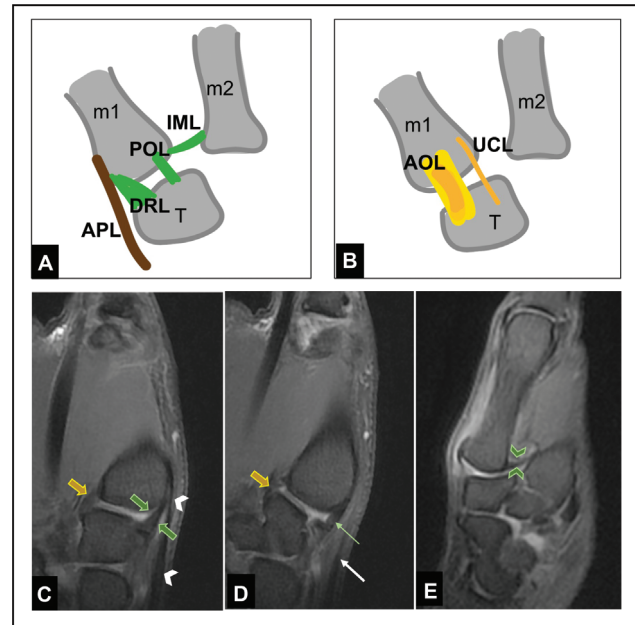


Fig. 5 Ligaments and tendons around the trapeziometacarpal joint. (A) Diagrammatic representation of thumb in coronal plane shows the components of dorsal first carpometacarpal ligaments. The dorsoradial ligament (DRL) is a capsular thickening between the dorsal surface of the trapezium (T) to the dorsoradial surface of the base of the first metacarpal (m1) deep to the abductor pollicis longus (APL) tendon. The posterior oblique ligament (POL) is also a capsular ligament between the trapezium and base of first metacarpal, positioned more ulnar to the attachment of the DRL. The intermetacarpal ligament (IML) extends from the ulnar side of the base of first metacarpal (m1) to the radial side of the base of the second metacarpal (m2). (B) Diagrammatic representation of thumb in coronal plane shows components of volar first carpometacarpal ligaments. The thicker anterior oblique ligament (AOL) has superficial and deep components, extending from the volar tubercle of trapezium (T) to the volar tubercle of the first metacarpal (m1). The ulnar collateral ligament (UCL) is a thinner ligament between the volar surface of the trapezium, near the attachment of the flexor retinaculum to the base of the first metacarpal and is often not well delineated on conventional magnetic resonance imaging (MRI). (C and D) Serial sagittal fat suppressed proton density (PDFS) MR image shows DRL (thick green arrow, C) deep to the APL (white arrow heads, C) and the AOL (yellow arrows, C and D). The POL (thin arrow) is seen, ulnar to DRL and is seen on the sagittal section where APL is no longer visible, but extensor pollicis tendon (white arrow) is seen. (E) The oblique coronal reformatted PDFS MR image of a different patient demonstrates the IML (green arrowheads).

and serve as the main stabilizer against hyperextension. There is a fibrocartilaginous pad, visible between the two SPLs that invest the sesamoid bones and is inseparable from the plantar capsule and above-described ligaments. The ligaments between the lateral and medial aspect of the proximal phalanx and the head of metatarsal are the lateral and medial collateral ligaments, respectively, that typically are not considered part of the “plantar plate complex” and protect against varus and valgus forces, respectively^{3,8} (→Figs. 6 and 7).

The musculo-tendinous complex provides dynamic stabilization to the joint. The flexor hallucis longus (FHL)

Table 3 Comparative analysis of the tarsometatarsal joint and the carpometacarpal joint

| | Great toe: Tarsometatarsal joint | Thumb: Carpometacarpal joint |
|-----------|---|--|
| Ligaments | Dorsomedial ligament (dC1-M1) Dorsal Lisfranc's ligament (dC1-M2) Dorsal intercuneiform ligament (dC1-C2) Plantar tarsometatarsal ligament (pC1-M1) Plantar Lisfranc's ligament complex (pC1-M2/M3) | Dorsal carpometacarpal ligament complex—DRL and POL Intermetatarsal ligament UCL-AOL |
| Tendons | At distal end of medial cuneiform: Peroneus longus Tibialis anterior At base of first metatarsal: Peroneus longus Tibialis anterior | At trapezium: Nil At base of first metacarpal: APL |

Abbreviations: AOL, anterior oblique ligament; APL, abductor pollicis longus; DRL, dorsoradial Ligament; POL, posterior oblique ligament; UCL, ulnar collateral ligament.

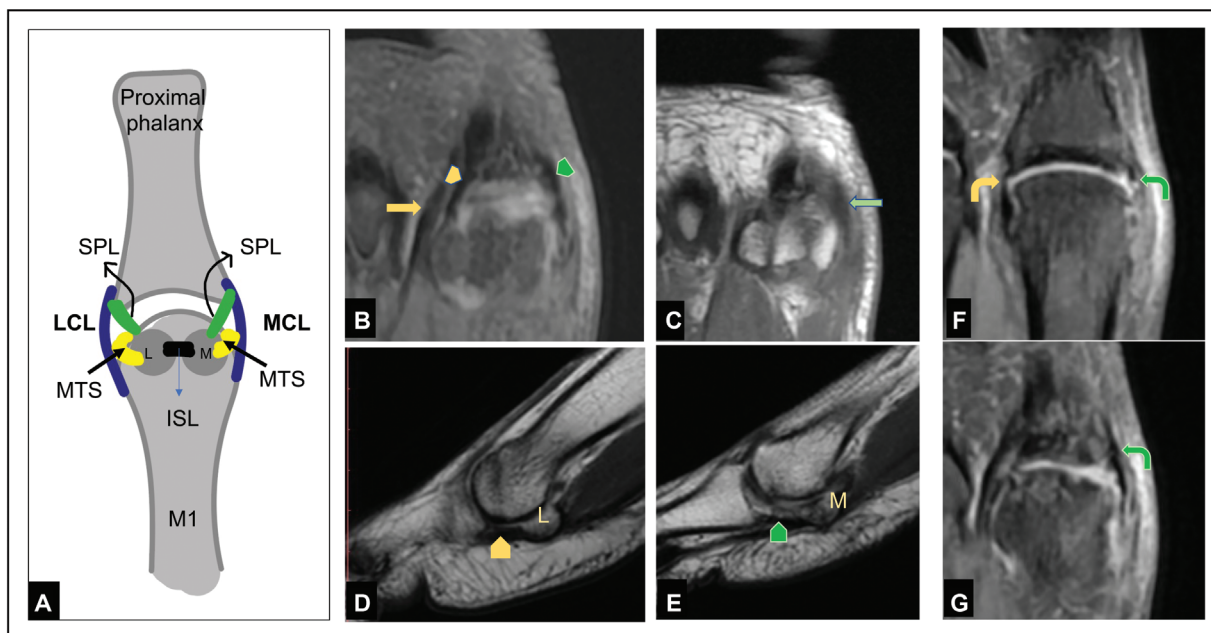


Fig. 6 Ligamentous attachments around the first metatarsophalangeal (MTP) joint representing the plantar plate complex. (A) Diagrammatic representation of the first MTP joint shows the medial (M) and lateral (L) sesamoids and their paired attachments to the plantar surface of the base of proximal phalanx—the sesamoidophalangeal ligaments (SPL), paired metatarsosesamoid ligaments (MSL) between the respective sesamoid and neck of first metatarsal. Medial (M) and lateral (L) collateral ligaments are obliquely oriented, from the head of metatarsal on each side to the plantar surface of the base of proximal phalanx. The intersesamoid ligament (ISL) is between the two sesamoids. (B) Axial fat suppressed proton density weighted (PDFS) magnetic resonance (MR) image and (D) sagittal T2-weighted imaging (T2WI) shows the lateral SPL (yellow arrow heads) as thick ligament extending from the lateral (L) sesamoid to the base of proximal phalanx, deep to the conjoint tendon of the adductor hallucis (yellow arrow). Similarly, (B) axial PDFS and (E) sagittal T2WI show the medial SPL (green arrow heads) as thick ligament extending from the medial (M) sesamoid to the base of proximal phalanx. (C) The subsequent T1W axial image shows the abductor hallucis (green arrow), which is superficial to the medial SPL. (F and G) Sequential PDFS axial MR image shows the medial collateral ligament (MCL) (bent green arrow) and lateral collateral ligament (LCL) (bent yellow arrow) extending from the base of proximal phalanx to the head of first metatarsal on each side. Note the discontinuity and preligamentous edema at the metatarsal attachment of MCL suggestive of a tear.

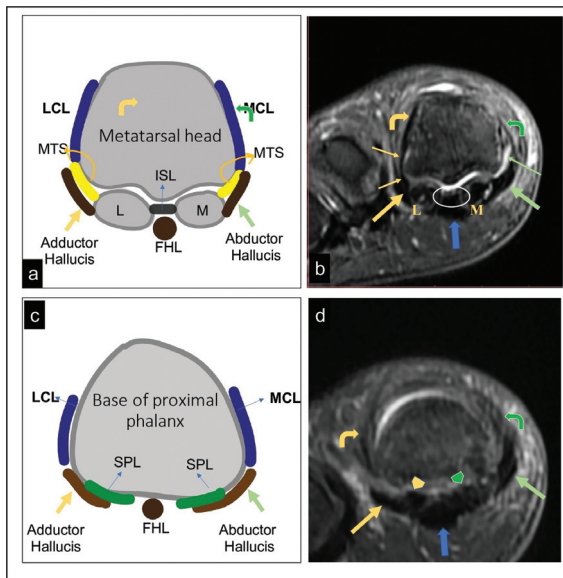


Fig. 7 Ligamentous attachments around the first metatarsophalangeal (MTP) joint. (A, C) Axial diagrammatic representation and (B, D) corresponding fat suppressed proton density (PDFS) axial magnetic resonance image at the level of first metatarsal head and base of proximal phalanx shows the medial collateral ligament (bent green arrows) and lateral collateral ligaments (yellow bent arrows). The lateral sesamoidophalangeal ligament (MTS, curved arrow in a, straight arrows in B) is seen extending between the lateral sesamoid and metatarsal head, merging with the collateral ligaments. The medial MTS ligament (curved green arrow in A) is seen between medial sesamoid and adjacent metatarsal head; the corresponding axial PDFS image (B) shows fluid signal (green arrow) and absence of T2 hypointense signal at the location of the ligament suggesting tear of the medial MTS ligament. The sesamoidophalangeal ligaments are seen at the level of base of proximal phalanx (C, D; medial—green arrowhead, lateral—yellow arrowhead). The adductor hallucis tendon (yellow arrow) and abductor hallucis tendon (green arrow) are seen superficial to the ligaments, ultimately merging with it.

tendon runs beneath ISL, in the groove between the two sesamoids and finally attaches to the base of the distal phalanx. The paired flexor hallucis brevis attaches to the respective sesamoid bones. On the medial aspect, abductor hallucis tendon attaches to the medial sesamoid with extensions to the capsule–ligamentous complex and medial aspect of the base of the proximal phalanx. Similarly, on the lateral aspect, conjoint tendon of the oblique and transverse heads of adductor hallucis attach to the lateral sesamoid with extensions to the capsule–ligamentous complex and lateral aspect of the base of the proximal phalanx^{3,8} (►Figs. 8 and 9).

On the dorsal aspect of the MTP joint, the extensor hallucis brevis and extensor hallucis longus (EHL) pass over the dorsal plate to finally attach on the dorsal aspect of the base of the proximal and distal phalanx, respectively. The extensor tendons are anchored to the underlying bones by the medial and lateral sagittal bands^{3,8} (►Fig. 10).

Thumb

The first MCP joint is also an ellipsoid joint that allows flexion, extension, limited adduction, abduction, rotation, and circumduction. Analogous to the plantar plate complex, there exists a similar “volar plate complex” comprising the radial and ulnar sesamoids, embedded within the fibrocartilaginous volar plate with a gamut of ligamentous and musculo-tendinous attachments. Its ligamentous support is less robust, allowing more mobility and less stability compared with the MTP joint that plays a pivotal role in weight bearing and walking.

The radial and ulnar collateral ligaments attach proximally on the volar aspect of the metacarpal head laterally and distally to the dorsolateral aspect of the base of the proximal phalanx. The accessory collateral ligaments attach to the

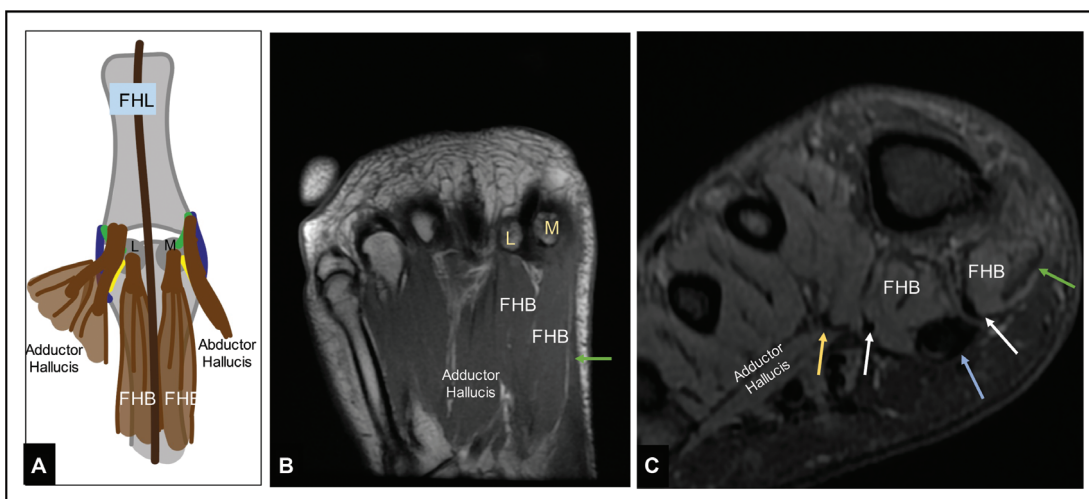


Fig. 8 Musculotendinous attachments around the first metacarpophalangeal (MCP) joint. (A) Diagrammatic representation and (B) corresponding axial T1-weighted magnetic resonance (MR) image show the adductor hallucis muscle attaching to the lateral sesamoid (L) and to the base of proximal phalanx and adjoining capsule–ligamentous complex (not shown here), the medial and lateral heads of the flexor hallucis brevis (FHB) attaching to the respective sesamoids, and the tendon of abductor hallucis (green arrow) is seen attaching to the medial sesamoid (M). (C) Coronal fat suppressed proton density MR image shows transverse head of adductor hallucis and its tendon (yellow arrow), lateral and medial FHB and its tendons (white arrows) and in the medial most aspect, tendon of abductor hallucis (green arrow).

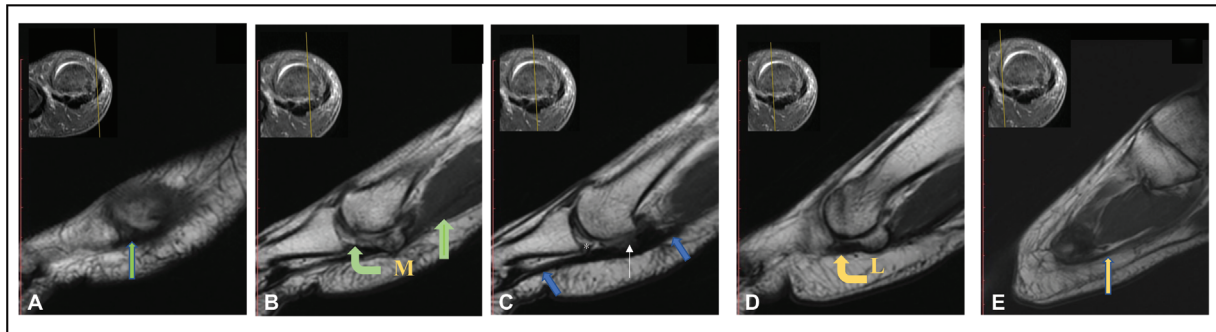


Fig. 9 Plantar plate complex. The serial sagittal T2-weighted magnetic resonance images show the components of the plantar plate complex of the first metatarsal joint with corresponding level of section (shown in the inset). (A) The medial most section shows attachment of the abductor hallucis (green arrow) to the medial sesamoid and capsuloligamentous structures attaching to the medial side of the base of the first metatarsal. (B) The next section shows medial sesamoidophalangeal ligament (SPL; bent green arrow) between the medial sesamoid (M) and plantar surface of the base of the base of the first proximal phalanx and the medial head of flexor hallucis brevis (FHB) attaching to the medial sesamoid (M). (C) The section through the midline of the metatarsophalangeal (MTP) joint, shows the flexor hallucis longus (FHL) tendon (blue arrows) passing over the fibrocartilage part of the plantar plate (white asterisk) and inseparable from the intersesamoid ligament (thin white arrow). (D) The sagittal section at the level of the lateral sesamoid (L) shows the lateral SPL (bent yellow arrow) between the lateral sesamoid (L) and plantar surface of the base of the base of the first proximal phalanx and the lateral head of FHB attaching to lateral sesamoid (L). (E) The lateral most section through the first MTP joint shows the conjoint tendon of adductor hallucis (yellow arrow) attaching to the lateral sesamoid, adjacent capsuloligamentous complex, and lateral surface of the base of proximal phalanx.

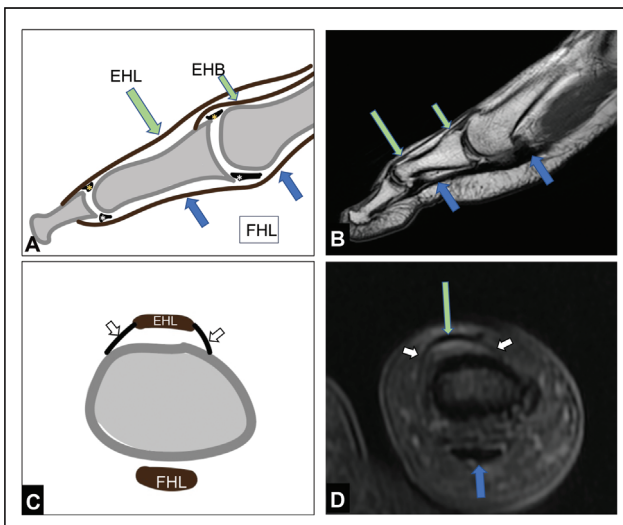


Fig. 10 Extensor and flexor compartment muscles of the great toe. (A) Sagittal schematic diagram and (B) sagittal fat suppressed proton density (PDFS) shows that the flexor hallucis longus (FHL) (blue arrows) attaches to the base of the distal phalanx on the plantar aspect, passing over the plantar plate of distal interphalangeal (DIP) and plantar plate complex of metatarsophalangeal (MTP) (white asterisks). The extensor hallucis brevis (EHB) (short green arrow) attaches to the dorsal aspect of the base of the proximal phalanx and the extensor hallucis longus (EHL) (long green arrow) goes on to attach on the dorsal aspect of the base of the distal phalanx, passing over the dorsal plates (yellow asterisks) at the level of intervening joints. (C) Axial schematic diagram and (D) corresponding axial PDFS magnetic resonance image at the level of proximal phalanx shows the EHL (green arrow) is secured to the underlying bone through thin sagittal bands (white arrows).

metacarpal head (volar to proper collateral ligaments), connecting it to the respective sesamoids and the volar plate^{6,9} (►Figs. 11 and 12).

The radial and ulnar sesamoids provide attachments to flexor pollicis brevis (FPB) and adductor pollicis, respectively. The aponeurosis of adductor pollicis extends further to attach on the ulnar aspect of the base of the proximal phalanx. The tendon of abductor pollicis brevis is however attached only to the radial aspect of base of proximal phalanx^{6,9} (►Figs. 11 and 12).

The flexor pollicis longus (FPL) tendon passes over the volar plate in the groove between the sesamoid bones to finally attach to the base of the distal phalanx (►Fig. 13). FPL is anchored to the underlying bones by the annular pulley system that prevents bow-stringing of the tendon during flexion. The pulley system of the thumb differs from the rest of the digits as there are no transverse pulleys, but only annular pulleys as described in ►Fig. 14.^{6,9}

Similar to the MTP joint, extensor pollicis brevis (EPB) and extensor pollicis longus (EPL) tendons pass over the dorsal plate of the MCP joint and finally attach to the dorsal aspect of the base of the proximal and distal phalanx, respectively (►Fig. 13). EPB, being a muscle of the first extensor compartment of the forearm, is visualized more radial to the EPL, a muscle of the third compartment. The extensor tendons are anchored to the underlying bones by the medial and lateral sagittal bands^{6,9} (►Fig. 15 and ►Table 4).

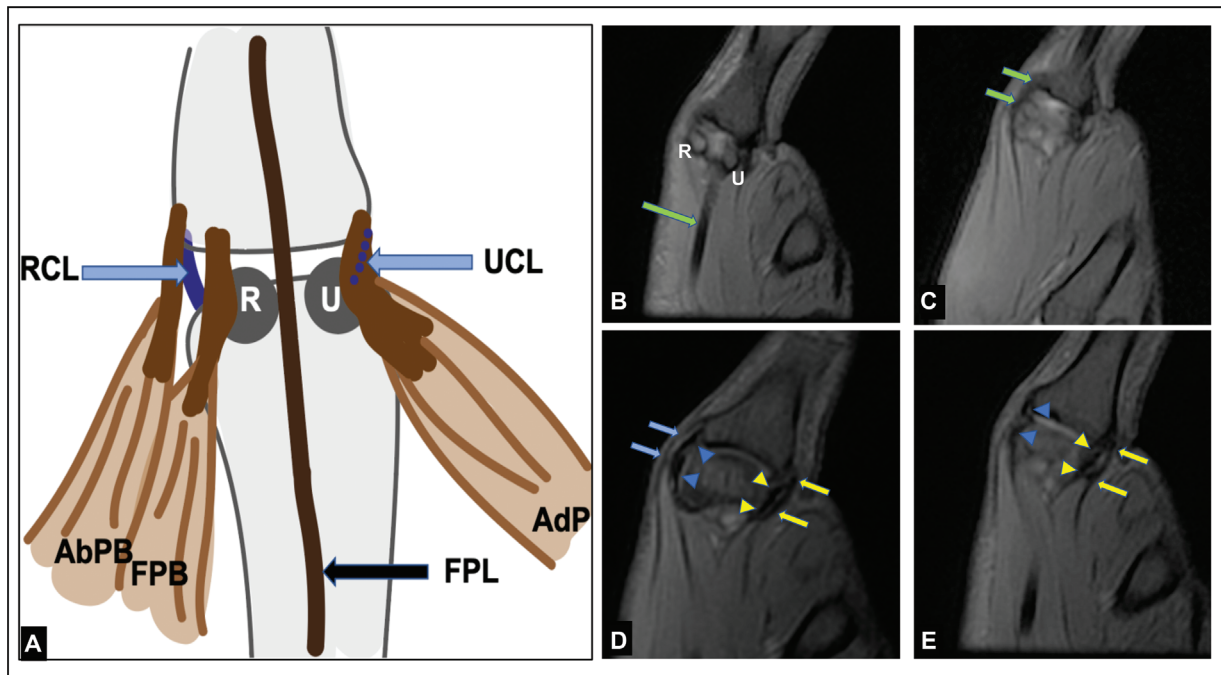


Fig. 11 Ligamentous and tendinous attachments around the first metacarpophalangeal joint (MCP). (A) Schematic diagram shows the ligamentous and tendinous attachments around the first MCP. The radial (RCL) and ulnar collateral ligaments (UCL) are seen extending obliquely from the palmar aspect of head of metacarpal to the base of proximal phalanx on the radial and ulnar aspect respectively. The adductor pollicis (AdP) attaches to the ulnar sesamoid (U), with aponeurotic extension to the base of proximal phalanx. While the tendon of flexor pollicis longus (FPL) passes across the MCP joint in between the two sesamoid bones, the flexor pollicis brevis (FPB) attaches on the radial sesamoid (R). The abductor pollicis brevis (AbPB) attaches directly to the base of radial aspect of proximal phalanx. (B–E) Serial coronal fat suppressed proton density magnetic resonance imaging showing the radial (R) and ulnar (U) sesamoid bones and FPL tendon (long green arrow) in (B). FHB tendon (short green arrows; c) is seen attaching on the radial sesamoid and base of proximal phalanx. The RCL (blue arrow heads; D–E) lies deep to the AbPB (blue arrows; D), whereas the UCL (yellow arrow heads; D–E) lies deep to the AdP aponeurosis (yellow arrows; D–E), attaching distally to the base of proximal phalanx on its radial and ulnar aspect, respectively.

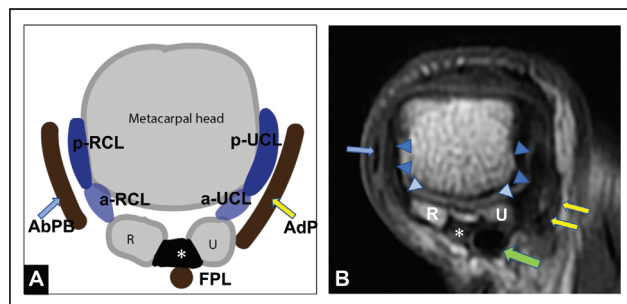


Fig. 12 Ligamentous and tendinous attachments around the first metacarpophalangeal (MCP) joint. (A) Schematic diagram and (B) axial T1-weighted imaging at the level of the head of the first metacarpal joint showing the ligamentous attachments around the first MCP joint. The proper radial (p-RCL, A; dark blue arrow heads, B) and proper ulnar (p-UCL, A; dark blue arrow heads, B) collateral ligament proximally attach to the metacarpal head, whereas the accessory radial (p-RCL, A; light blue arrow heads, B) and accessory ulnar (a-UCL, A; light blue arrow heads, B) collateral ligaments attach to the radial (R) and ulnar (U) sesamoid bones, respectively. The volar plate (asterisk) is between the two sesamoid bones, with the flexor pollicis longus (FPL) tendon running along its volar aspect. The abductor pollicis brevis tendon (AbPb, blue arrow) and the adductor pollicis aponeurosis (AdP, yellow arrows) lie superficial to the respective collateral ligaments, attaching distally to the base of the proximal phalanx (not shown).

Interphalangeal Joints

The IP joint in both great toe and thumb is a hinge joint, allowing only flexion and extension movement.

Paired collateral ligaments are present on the medial and lateral aspect of the joint extending between the distal end of proximal phalanx to the base of the distal phalanx. The respective EPL/EHL and FPL/FHL attach to the base of the distal phalanx of the dorsal and volar/plantar aspect, respectively. The volar/plantar plates and dorsal plates are also present at the IP joint that allow the tendons to glide over smoothly⁹ (► Figs. 16 and 17) (► Table 5).

Conclusion

The evolutionary development of human limbs facilitated their feet and hands to assume functional roles of stability and mobility, respectively, and hence they have many similarities with few dissimilarities in their anatomy. Evaluating their MRI anatomy in correlation allows a comprehensive understanding to a radiologist, enabling them to develop a systematic approach to read the MRI scans thereof.

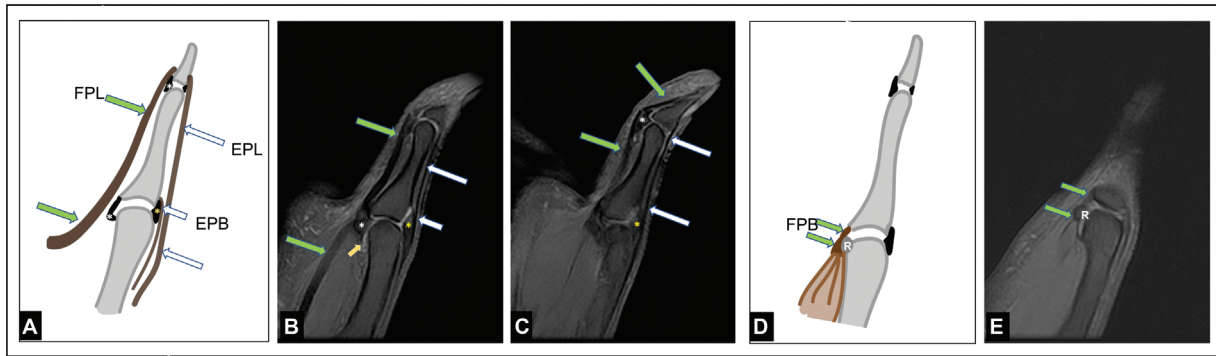


Fig. 13 Muscles of the flexor and extensor compartment of the great toe. (A) Sagittal schematic diagram and (B, C) serial sagittal fat suppressed proton density (PDFS) shows that the flexor pollicis longus (FPL; green arrows) attaches to the base of the distal phalanx on the volar aspect, passing over the volar plates (white asterisks) at the level of metacarpophalangeal (MCP) and distal interphalangeal (DIP) joints. The extensor pollicis brevis (EPB; short white arrow) attaches to the dorsal aspect of the base of the proximal phalanx and the extensor pollicis longus (EPL) (long white arrow) goes on to attach on the dorsal aspect of the base of the distal phalanx, passing over the dorsal plates (yellow asterisks) at the level of intervening joints. Note that there is a synovial recess (yellow arrow, B) at the proximal attachment of the volar plate, which should not be misinterpreted as a tear. (D) Sagittal schematic diagram and (E) serial sagittal PDFS shows the attachment of the flexor pollicis brevis (FPB; short green arrows) on the radial sesamoid (R) and volar aspect of the base of proximal phalanx.

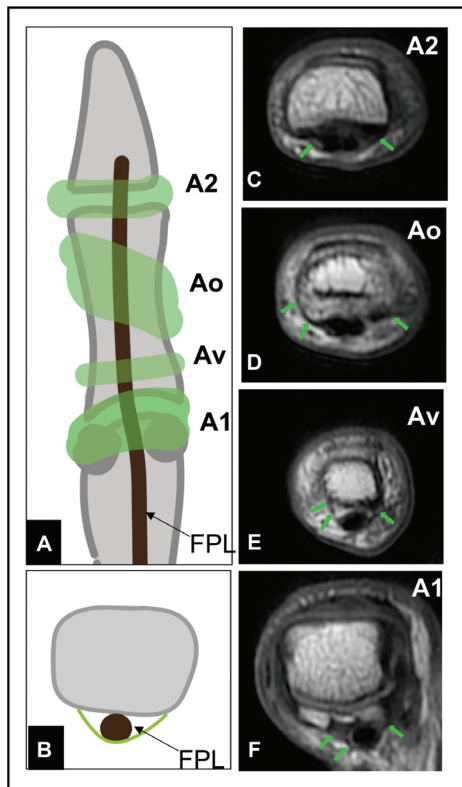


Fig. 14 Pulley system around the flexor pollicis longus (FPL) tendon. (A) Coronal schematic diagram showing the positions of annular pulleys (shaded in green): A1 and A2 are along the metacarpophalangeal (MCP) and distal interphalangeal (DIP) joints, respectively. The oblique pulley (Ao) is along the diaphysis of proximal phalanx and oriented obliquely. The variable pulley (Av) is between the A1 and A2. (B) Axial schematic diagram showing the position of annular pulleys in relation to the FPL tendon. The pulleys (green line) surround the FPL tendon, attaching to the palmar aspect of the phalanges, preventing bowstringing of FPL. (C–F) Corresponding axial magnetic resonance T1-weighted images are shown in the panel on the right with the pulleys marked with green arrows. To merge either A1 and A2 pulleys are seen to merge with the underlying volar plates.

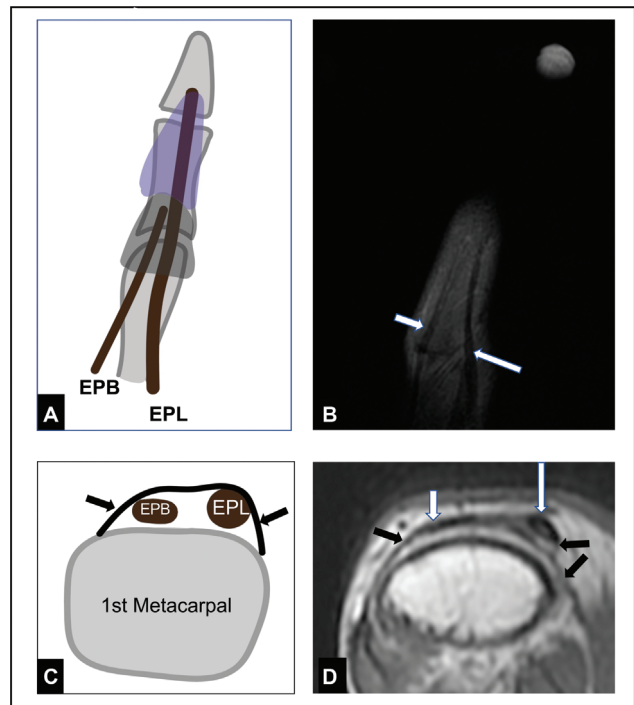


Fig. 15 Extensor muscles of the thumb. (A) Coronal and (C) axial schematic diagram. (B) coronal fat suppressed proton density magnetic resonance (MR) images and (D) axial T1-weighted MR images at the level of first metacarpal bone show that the extensor pollicis brevis (EPB, short white arrow) lies radial to the extensor pollicis longus (EPL, long white arrow). Note that even at the level of distal forearm and wrist, the EPB is more on the radial aspect as it belongs to the first compartment and EPL belongs to the third compartment of the extensor group of muscle. The tendons are held in central position by the sagittal bands (shaded in gray in a, black arrows in C–D), in and around the metacarpophalangeal (MCP) joint, whereas more distally, it is supported by a faint triangular expansion (shaded in purple), which is not well appreciated on imaging.

Table 4 Comparative analysis of the first metatarsophalangeal (MTP) joint of foot and metacarpophalangeal (MCP) joint of thumb

| | Great Toe: First MTP joint | Thumb: First MCP joint |
|-----------|--|--|
| Ligaments | Plantar plate—fibrocartilage pad ^a Medial and lateral SPL ^a Intersesamoid ligament ^a MCL LCL Medial and lateral MTSL ^a Dorsal plate Medial and lateral sagittal bands | Volar plate Intersesamoid ligament RCL UCL supported by adductor aponeurosis Accessory UCL and RCL Dorsal plate Radial and ulnar sagittal bands Pulleys |
| Tendons | Lateral sesamoid: FHB (lateral head), adductor hallucis Medial sesamoid: FHB (medial head), abductor hallucis FHL EHL EHB | Ulnar sesamoid: adductor pollicis Radial sesamoid: FPB Base of first metacarpal radial aspect: abductor pollicis brevis FPL EPL EPB |

Abbreviations: EHB, extensor hallucis brevis; EHL, extensor hallucis longus; EPB, extensor pollicis brevis; EPL, extensor pollicis longus; FHB, flexor hallucis brevis; FHL, flexor hallucis longus; FPL, flexor pollicis longus; LCL, lateral collateral ligament; MCL, medial collateral ligament; MTSL, metatarsosesamoid ligament; RCL, radial collateral ligament; SPL, sesamoidophalangeal ligament; UCL, ulnar collateral ligament.

^aForms part of the “planter plate complex.”

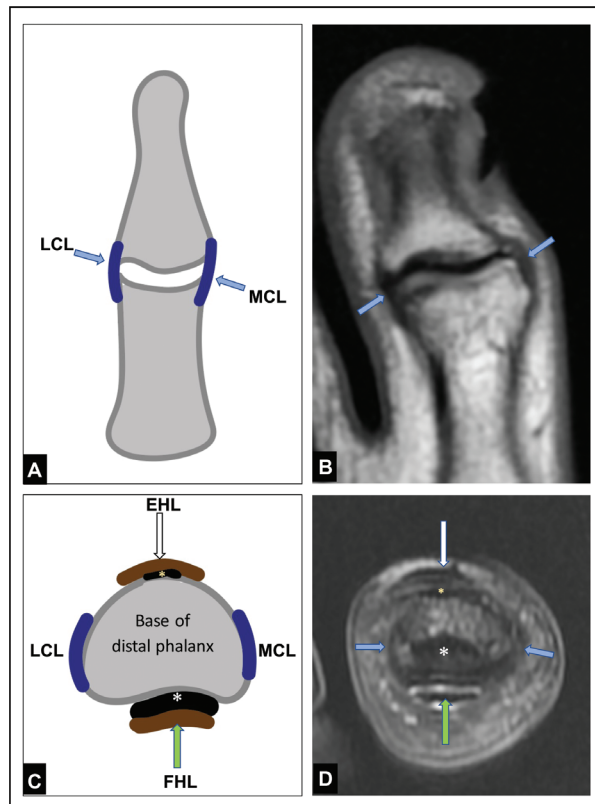


Fig. 16 Ligamentous and tendinous attachments near the distal interphalangeal (DIP) joint of the great toe. (A) Coronal schematic diagram and (B) coronal fat-suppressed proton density (PDFS) magnetic resonance (MR) image at the level of DIP joint show the lateral (LCL) and medial (MCL) collateral ligaments (blue arrows) extending from the lateral and medial aspects of distal end of proximal phalanx to the proximal end of distal phalanx, respectively. (C) Coronal schematic diagram and (D) axial PDFS MR image at the level of base of distal phalanx show LCL and MCL (blue arrows), extensor hallucis longus (EHL; long white arrow) and flexor hallucis longus (FHL; long green arrow) attached to the dorsal aspect and volar aspect respectively. The prominent volar plate is deep to the FHL tendon and is marked with white asterisk. The dorsal plate (yellow asterisk) is small.

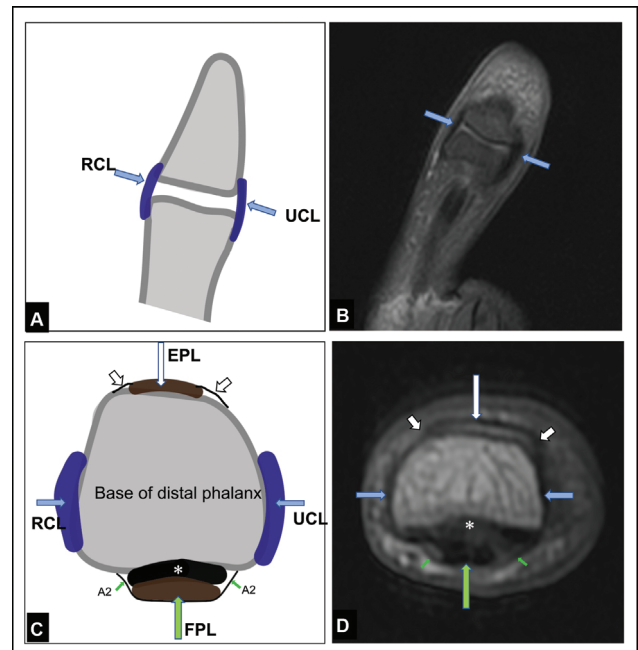


Fig. 17 Ligamentous and tendinous attachments near the distal interphalangeal (DIP) joint of the thumb. (A) Coronal schematic diagram and (B) coronal fat-suppressed proton density (PDFS) MR image at the level of DIP joint show the radial (RCL) and ulnar (UCL) collateral ligaments (blue arrows) extending from the radial and ulnar aspects of distal end of proximal phalanx to the proximal end of distal phalanx, respectively. (C) Axial schematic diagram and the (D) axial PDFS MR image at the level of base of distal phalanx show the radial and ulnar collateral ligaments (blue arrow) attached laterally, extensor pollicis longus (EPL; long white arrow) and flexor pollicis longus (FPL; long green arrow) attached to the dorsal aspect and volar aspect, respectively. The prominent volar plate is deep to the FPL tendon and is marked with white asterisk, while the A2 (small green arrows) pulley covers the FPL on its superficial aspect. The sagittal bands (small white arrow) are thin linear bands that secure the EPL tendon.

Table 5 Comparative analysis of interphalangeal (IP) joints of great toe and thumb

| | Great toe: IP joint | Thumb: IP joint |
|-----------|---|---|
| Ligaments | MCL LCL Plantar plate Dorsal plate | RCL UCL Volar plate Dorsal plate |
| Tendons | FHL EHL | FPL EPL |

Abbreviations: EHL, extensor hallucis longus; EPL, extensor pollicis longus; FHL, flexor hallucis longus; FPL, flexor pollicis longus; LCL, lateral collateral ligament; MCL, medial collateral ligament; RCL, radial collateral ligament; UCL, ulnar collateral ligament.

Conflicts of Interest

None declared.

References

- Ivanenko YP, Wright WG, St George RJ, Gurfinkel VS. Trunk orientation, stability, and quadrupedalism. *Front Neurol* 2013;4:20
- Biesecker LG, Aase JM, Clericuzio C, Gurrieri F, Temple IK, Toriello H. Elements of morphology: standard terminology for the hands and feet. *Am J Med Genet A* 2009;149A(01):93–127
- Stoller D. *Magnetic Resonance Imaging in Orthopaedics and Sports Medicine*. 3rd edition. Philadelphia: Lippincott Williams & Wilkins; 2007:677–680
- Siddiqui NA, Galizia MS, Almusa E, Omar IM. Evaluation of the tarsometatarsal joint using conventional radiography, CT, and MR imaging. *Radiographics* 2014;34(02):514–531
- Castro M, Melão L, Canella C, et al. Lisfranc joint ligamentous complex: MRI with anatomic correlation in cadavers. *AJR Am J Roentgenol* 2010;195(06):W447–55
- Rawat U, Pierce JL, Evans S, Chhabra AB, Nacey NC. High-Resolution MR. High-resolution MR imaging and US anatomy of the thumb. *Radiographics* 2016;36(06):1701–1716
- Cardoso FN, Kim HJ, Albertotti F, Botte MJ, Resnick D, Chung CB. Imaging the ligaments of the trapeziometacarpal joint: MRI compared with MR arthrography in cadaveric specimens. *AJR Am J Roentgenol* 2009;192(01):W13–9
- Hallinan JTPD, Statum SM, Huang BK, et al. High-resolution MRI of the first metatarsophalangeal joint: gross anatomy and injury characterization. *Radiographics* 2020;40(04):1107–1124
- Hirschmann A, Sutter R, Schweizer A, Pfirrmann CW. MRI of the thumb: anatomy and spectrum of findings in asymptomatic volunteers. *AJR Am J Roentgenol* 2014;202(04):819–827